



Published in final edited form as:

*Anal Chem.* 2012 November 6; 84(21): 8900–8908. doi:10.1021/ac3012945.

## 1-D and 2-D Photonic Crystals as Optical Methods for ‘Amplifying’ Biomolecular Recognition

Sudeshna Pal<sup>1,4</sup>, Philippe M. Fauchet<sup>1,3</sup>, and Benjamin L. Miller<sup>2</sup>

Benjamin L. Miller: Benjamin\_Miller@urmc.rochester.edu

<sup>1</sup>Department of Electrical and Computer Engineering, University of Rochester, Rochester, New York 14642

<sup>2</sup>Department of Dermatology, University of Rochester, Rochester, New York 14642

<sup>3</sup>Department of Electrical Engineering and Computer Science Vanderbilt University, Nashville, Tennessee 37235

<sup>4</sup>Department of Mechanical, Materials, and Aerospace Engineering University of Central Florida, Orlando, Florida 32816

### Abstract

Label-free sensing strategies are an intensely studied and increasingly used alternative to signal amplification via fluorescent labels and enzymatic methods. This article discusses one class of optical sensors, termed “photonic crystals”, that effectively amplify binding events (such as analyte capture) via strong light-matter interactions.

### Introduction

Because we humans lack the ability to directly sense and distinguish individual organisms and most nonvolatile molecules of biomedical interest at physiologically relevant concentrations, medical diagnostics have generally required some sort of amplification step in order to produce useful output. This amplification can take many forms. At the organism level, the number of bacteria or viruses can be amplified through culture, allowing direct visualization of colonies on an agar plate, or as a Gram stain under the microscope.<sup>1</sup> A transformative development in the late 20<sup>th</sup> century was the discovery that the polymerase chain reaction and related processes can physically amplify the amount of a DNA or RNA sequence present in a sample, simplifying their subsequent detection.<sup>2</sup> Proteins, of course, generally cannot be physically amplified in a PCR-like process. In the early days of immunoassay, amplification was provided by radioactive labels. These techniques have been augmented by enzymatic and fluorescence-based strategies, which dominate modern immunodiagnostics.<sup>3</sup> All of these methods, however, increase the time, cost, complexity, and potential for error (human and otherwise) needed for assay. Thus, “label-free”, direct-sensing methods of biodetection have become increasingly important, and a major area of research in recent years.<sup>4</sup>

The designation “label-free” should not necessarily be read as an implication that amplification is no longer needed, or no longer occurs, however. Now, rather than amplifying the material being sensed (by increasing its copy number enzymatically, or using a secondary reporter of some type that provides an increased chemical signal), researchers are designing novel materials and novel material configurations in which the interaction of a

captured analyte with the optical field of the sensor is generally detectable via a change in the spectrum produced by the device. This may be viewed as an optical “amplification” of the captured analyte. This article discusses one such class of structures, in which specific material types and configurations called “photonic crystals” are employed to amplify an optical field interacting with a binding event. First introduced conceptually in 1987,<sup>5,6</sup> photonic crystals (PhCs) are devices that incorporate alternating regions of high refractive index contrast in a periodic array of 1, 2, or 3 dimensions (Figure 1). PhCs can be designed to have a photonic band gap (PBG), or “stop band”, where light for a range of frequencies falling within the PBG cannot propagate through the crystal structure. Put another way, if the periodic array is effectively infinite (in practice, a small array can provide very high performance), light couples in to the device, but no light at the frequencies defined by the PBG exits.

PhCs often incorporate an imperfection in their perfect periodicity known as a “defect”. This allows light of a particular wavelength to escape the PhC and act as a reporter for what goes on inside the device. This structure is also described as a “microcavity” or “nanocavity”. Concentration of the electromagnetic field in the region of the defect is one way PhCs amplify a sensing event. Subtle refractive index changes in the environment of the defect, such as those that occur on binding a molecular target, produce a measurable shift of the wavelength that is transmitted through the PhC.

In principle, PhCs can provide extraordinary sensitivity: for example, preliminary experiments suggest that single virus particle detection should be possible for 2-D PhCs, assuming that one can successfully deliver that single virus particle to the active sensing area. Their small size (active sensing region as small as a 100 nm diameter cylinder) and the compatibility of semiconductor materials-based PhCs with fabrication protocols developed in the microelectronics industry make them exceptionally suitable for integration into “lab on a chip” devices. This article will highlight several examples of sensors based on 1- and 2-D PhCs, and their prospects for evolving into production-scale biosensors and diagnostics. Although 3-D PhCs have been fabricated, as far as we are aware they have not yet been used in a sensing context.

## 1-D PCs in Biosensing

The potential utility of PhC structures in biosensing was first demonstrated a little over a decade ago via 1-D PhC devices fabricated in porous silicon (PSi).<sup>8</sup> Initially explored in the 1950s by Ulhir<sup>9</sup> and Turner,<sup>10</sup> and later by Canham and colleagues,<sup>11</sup> porous silicon is readily produced by electrochemical etching of n- or p-type bulk silicon. By modifying the etch conditions, including the etchant solution and current density, both the pore size and porosity of the resulting material can be precisely controlled. Since etching occurs most rapidly at the interface between the etchant solution and un-etched (bulk) silicon, one can produce complex three-dimensional structures in porous silicon by varying the current density as a function of time. For example, alternating cycles of high and low current density yield devices with regularly spaced regions of high and low porosity (as shown in Figure 1). This structure functions as a 1-D PhC, or Bragg mirror. Changes in the edge frequency of the stop band produced by the Bragg mirror can be used as a reporter for target binding. Alternatively, fabrication of a microcavity via incorporation of a defect layer produces a sharp and readily observable peak (or set of peaks) within the stop band. By carefully controlling the etch process, one can readily produce microcavities of very high quality.

While many experiments with porous silicon have relied on the reflected signal,<sup>12</sup> our earliest efforts focused on the ability of mesoporous silicon (pore diameters in the range of 2 to 50 nm) to provide room-temperature photoluminescence.<sup>13</sup> Like the transmission or

reflectance spectrum, the photoluminescence spectrum of a microcavity can be modulated by the presence of an analyte of interest. Importantly, the position of photoluminescence peaks is relatively insensitive to temperature variation within the typical ambient laboratory environment.<sup>14</sup> Initial experiments demonstrated that PSi 1-D PhCs functionalized with oligonucleotides complementary to genomic DNA from lambda bacteriophage allowed selective detection of the virus, visible as a red shift in the photoluminescence spectrum.<sup>15</sup> The versatility of these label-free sensors (both with regard to the types of targets towards which they could be applied, as well as the range of capture molecules that could be incorporated into them) was shown in 2001,<sup>16</sup> in experiments using a PSi 1-D PhC onto which a synthetic receptor we designed<sup>17</sup> for bacterial diphosphoryl lipid A had been immobilized. This device successfully differentiated Gram(-) bacteria, which have considerable amounts of lipid A in their outer cell membranes, from Gram(+) bacteria, which do not. Since these initial proof-of-concept experiments, we have shown that PSi PhCs can be fabricated in such a way so as to allow infiltration of large (protein size) molecules,<sup>18</sup> and can even be incorporated into a hydrogel bandage material.<sup>19</sup> In the latter case, we found that the gel-immobilized device could be subjected to repeated cycles of drying and rehydration for more than a year without losing sensing capability.

Two reports from the DeLouise group provide particularly encouraging data with regard to the future of porous silicon-based devices in the diagnostics field.<sup>20,21</sup> Using a PSi 1-D Bragg mirror, the authors constructed a sensor for morphine and morphine metabolites. To enable sensitive detection of these low molecular weight species, the authors first immobilized a morphine derivative on the PSi sensor. Application of a urine sample to which an anti-morphine antibody had been added allowed quantitative detection of morphine at concentrations ranging from 18.0 nM to 10.8 μM via a competitive binding mechanism. The authors observed a maximum red-shift of  $6.0 \pm 0.7$  nm in blank urine containing an anti-morphine antibody; the lower limit of detection was established based on the spectrometer resolution of 0.06 nm/pixel. Subsequently, head to head comparison of the performance of this sensor with a reference standard clinical assay (LC-MS/MS) showed a 96% concordance across 50 patient samples. This work represents an important milestone in the evolution of PSi 1-D PhCs from laboratory research project to robust clinically-applicable technology.

PhC biosensors are not limited to monolithic structures, however. Two of the many novel applications of porous silicon 1-D PhCs described by the Sailor group are “smart dust” (small rugate filter-encoded porous silicon fragments able to carry out sensing while dispersed in solution<sup>22</sup>), and the use of double-layer porous silicon devices as monitors for the progress of enzymatic reactions.<sup>23</sup> In the latter device, shifts in the reflectivity spectrum as a function of trapped reaction product provide a real-time optical readout. Porous silicon PhC microparticles have also been described by the Gooding group,<sup>24</sup> with the goal of developing homogeneous single-cell sensing systems.<sup>25</sup>

Other materials systems can also be used for the production of 1-D PhCs. For example, a 1-D-PhC based sensor in total-internal-reflection (TIR) geometry has been developed using alternating layers of TiO<sub>2</sub> and SiO<sub>2</sub> deposited by an electron-beam physical vapor method.<sup>26,27</sup> This device could be operated in a continuous flow mode, allowing real-time detection of DNA, proteins and antibodies with a refractive index sensitivity on the order of 10<sup>-8</sup> refractive index unit (RIU). Planar 1-D PhCs arrayed along a bus waveguide on silicon have also been demonstrated.<sup>28</sup>

Polymers can also be used to make 1-D PhCs. Use of polymers permits simple, large-scale sensor fabrication and detection schemes, including incorporation into microarray, microplate, and microfluidic formats. As a result, these structures have therefore been

explored extensively in both the academic and commercial realms. Both 1D and 2D PhC designs have been employed by the Cunningham group in out-of-plane sensing.<sup>29</sup> Their PhC structures are made from a low-RI (typically polyethylene terephthalate,  $n=1.45$ ) polymer substrate having subwavelength periodic modulations on its surface, overcoated with a high-RI ( $n=2.0$ ) dielectric coating (usually a layer of  $\text{TiO}_2$ , although early work also employed silicon nitride<sup>30</sup>). Use of nano-replica molding of plastic materials in the fabrication process allows such substrates to be produced inexpensively in large volumes. When the PhC surface is illuminated with TM white light, the reflectance spectrum shows a sharp resonance peak (shown schematically in Figure 3a). The sensing mechanism relies on shifts of the reflected resonance peak due to RI changes in the surrounding medium. Using this PhC design, detection of biomolecules such as proteins and DNA as well as larger targets such as live cells and viruses has been demonstrated, providing a sensitivity for dried protein layers on the order of  $0.4 \text{ pg/mm}^2$ .<sup>31,32,33,34</sup> SRU Biosystems' BIND<sup>35</sup> and the Corning EPIC system<sup>36</sup> are two examples of commercial products employing out of plane 1-D PhC technology. A particularly interesting application of the EPIC system has been in monitoring the redistribution of cellular components during whole-cell assays.<sup>37</sup> The BIND sensor has been employed in (among others) high-throughput screening of putative inhibitors of protein-protein (Figure 3c<sup>38</sup>) and protein-DNA<sup>31</sup> interactions. These devices have also been used in combination with fluorophore labeling to produce a "PhC enhanced fluorescence" sensor, effectively providing amplification (via the PhC) of an amplifier (the fluorophore).<sup>39</sup> Alternatively, a high SERS (surface enhanced Raman scattering) signal may be achieved by coating the surfaces with a high density of electrically isolated Ag nanoparticles.<sup>40</sup>

## The current frontier: 2-D PhCs in biosensing

With the 1-D PhC well established in a laboratory setting and beginning to find commercial application, researchers have begun to explore the design, fabrication, and applications of 2-D PhCs. 2-D PhCs have several potential advantages. For example, 2-D PhC nanocavities can be manufactured with active sensing regions on the order of a few hundred  $\text{nm}^2$ , and sensitivities approaching the single-molecule or single virus particle level.

In 2-D PhCs, the PBG appears for light that propagates within the plane of periodicity. This light can be separated into two independent polarizations: the transverse-electric (TE) and the transverse-magnetic (TM).<sup>41</sup> For TE modes, the magnetic field is normal to the plane of periodicity and the electric field is in plane, while the reverse is the case for TM modes. 2-D PhCs studied to date generally fall in to one of two common configurations: a square lattice of high refractive index rods surrounded by a low index medium, and a hexagonal lattice of low index holes embedded in a high index medium. 2-D PhC based detection methodologies can be broadly classified into two geometries, enabling in-plane and out-of-plane sensing.

Since infinitely thick materials do not exist in the real world, realization of 2-D PhC structures for in-plane sensing has mostly been in the form of thin PhC slabs, such as those that can be made from silicon-on-insulator (SOI) substrates using electron-beam lithography and reactive-ion etching.<sup>42</sup> Light confinement in the 2-D PhC slabs occurs horizontally through the PBG and vertically through total internal reflection (TIR) within the slab due to the high refractive index contrasts between the slab and its surroundings. The slab thickness in 2-D PhCs plays a crucial role in determining the existence and size of the PBG in these structures. PhC slabs with a half-wavelength thickness are well suited for confining the fundamental mode, as well as preventing higher-order modes. Dimensions less than 100 nm are necessary for near-infrared wavelength applications, a convenient wavelength range for silicon-based devices. A typical fabrication process begins by coating the SOI wafer with a layer of poly-methyl-methacrylate (PMMA), an electron-beam sensitive resist. Electron-beam lithography is used to directly write the PhC patterns on the SOI wafers, and then the

pattern is transferred to the underlying silicon device layer by dry reactive-ion-plasma etching. Alternatively, if the Si etcher is not compatible with PMMA, the pattern may be transferred to an intermediate hard mask layer, usually silicon dioxide or silicon nitride, which acts as a mask for etching the device layer. Finally, the PMMA resist is stripped off. To obtain suspended PhC slabs for even higher refractive index contrast, the silicon dioxide box layer underlying the PhC can be removed using a timed wet etch process in aqueous hydrofluoric acid (HF) solution. Although not yet explored in a biosensing context, 2-D PhCs have also been fabricated in GaAs.

Further localization of light in 2-D PhCs is achieved by introducing defects in the crystal lattice. Point defects are created by perturbing a single lattice site (for instance by increasing or decreasing the radius of a central hole in a hexagonal lattice of air holes), which creates a single localized mode or a set of closely spaced modes having frequencies within the PBG. This is described as a microcavity (by analogy to the 1-D PhC microcavities described above), or “nanocavity”, by virtue of the exceptionally small device size. Alternatively, modifying a linear sequence of lattice sites (i.e. a linear defect) creates a 2-D PhC waveguide that allows modes to be guided through the crystal within its PBG. As with PhC nanocavities, light can also be localized in PhC waveguides by placing a point defect in the vicinity of the waveguide. Designing 2-D PhCs and understanding their performance are facilitated by two popular computational methods: the plane-wave expansion method (PWEM) and the finite-difference-time-domain method (FDTD).<sup>42</sup> PWEM directly computes the eigenstates and eigenvalues of Maxwell’s equations in a periodic structure, in a Fourier space. The FDTD method numerically integrates Maxwell’s equations in the time domain in a discretized, finite-difference form. Discretization is used in both time and space coordinates. The FDTD method is considered to be most applicable for PhC structures and is robust and simple to implement. FDTD simulations of the electric field confinement in two representative types of PhC microcavities are shown in Figure 4.

The light trapping efficiency in optical microcavities is characterized by two parameters: the quality factor  $Q$ , and the mode volume  $V_m$  of the cavity. The  $Q$  is proportional to the length of time that the electromagnetic mode stays inside the cavity and is defined by:

$$Q = \frac{\omega E}{P}$$

where  $E$  is the energy stored inside the cavity,  $\omega$  is the resonant frequency and  $P$  is the power dissipating out from the cavity. The mode volume  $V_m$  represents the amount of space in which the electric field is resonantly enhanced by photon confinement.<sup>43</sup> PhC microcavities have been fabricated with both reasonably high  $Q$  ( $10^2$  to  $10^6$  for Si,  $> 10^6$  for GaAs) and low  $V_m$  (order of  $(\lambda/n)^3 \sim 0.035$  to  $0.085 \mu\text{m}^3$ ).<sup>44</sup> Although some of these  $Q$  values are lower than those attainable with ring resonators<sup>45</sup> and other “whispering gallery mode” structures,<sup>46</sup> interaction of a target analyte with the electric field (light) confined in a small area of the device causes a strong light-matter interaction which may be easily detected. 2D PhCs are also highly flexible from a design standpoint, as one can easily fabricate devices with different cavity sizes, allowing light to be confined at different resonance wavelengths inside the PhC. Changing the defect size also potentially allows size-based selection of targets.

An early demonstration of the use of 2D PhC nanocavities for simple refractive index sensing was described in 2004.<sup>47</sup> Sensors showed a resonance wavelength shift of approximately 0.4 nm for a refractive index (RI) change of 0.002 when the device was exposed to liquids with different refractive indices. *In-situ* time resolved sensing was also

demonstrated with a glycerol-water mixture. Other early work demonstrating the use of 2D PhCs for refractive index sensing included the use of coupled PhC arrays formed by periodically modifying holes of a square lattice photonic crystal slab, for example, by removing every third hole in both x and y directions. The defect modes of these individual cavities form coupled bands (monopole, dipole and quadrupole) located inside the PhC bandgap of the surrounding PhC. The structure showed strong dependence of the transmitted and reflected light on the input polarization, following the equation:

$$Intensity \propto \sin^2\left(\frac{2\phi\pi}{180}\right)$$

where  $\phi$  is the polarization angle. The position of resonance in the reflected signal was strongly dependent on the surrounding refractive index. These structures were fabricated on SOI substrates.<sup>48,49</sup>

Application of 2D PhC nanocavities to biomolecular detection was first reported in 2007.<sup>50</sup> The PhC structure employed in detection consisted of a hexagonal array of cylindrical air holes with the PhC lattice constant of 465 nm and an air hole diameter of 270 nm. A small defect was created by reducing the diameter of a central air hole to 140 nm. The PhC structures were fabricated on SOI chips with a 400 nm-thick Si slab separated from the Si substrate by a 1  $\mu\text{m}$  thick  $\text{SiO}_2$  box layer. The operating resonance wavelength of the structure was 1.58  $\mu\text{m}$  for TE-like modes. Two tapered ridge waveguides were used to couple light in and out of the cavity. For optical characterization, TE polarized light from a laser source (tunable from 1440 to 1590 nm) was coupled into the tapered ridge waveguide using a polarization-maintaining tapered lensed fiber. The transmitted signal was measured using an InGaAs (Indium Gallium Arsenide) detector.

Covalent capture of bovine serum albumin on a glutaraldehyde-functionalized surface was first performed as a simple demonstration of sensor response (Figure 4a). Examination of spectral shifts based on covalent capture of bovine serum albumin suggested capture of as little as 2.5 fg of analyte in the active area of the sensor could produce a measurable signal. Selective detection of streptavidin on an immobilized biotin layer was also demonstrated. Modification of the design of this structure to incorporate a defect diameter of 685 nm led to an experimentally realized device with an active sensing volume of 0.15  $\mu\text{m}^3$  (a solution volume of 0.15 femtoliters) and an experimental  $Q$ -factor of 2000.<sup>51</sup> With this device, infiltration of a single 370 nm diameter latex sphere could be detected. Nanoparticle infiltration into the defect, observed based on a sensor resonance red-shift of approximately 4 nm, was confirmed by scanning electron microscopy (SEM). The efficiency of nanoparticle capture was not reported. Real-time detection of protein targets using a similar device operating under flow has been described.<sup>52</sup>

## PhC Waveguides

While the 2-D PhC nanocavities described in the previous paragraph show promise for the ultrasensitive detection of single targets, it is not possible to place them in series along a waveguide (i.e. for multiplex detection) since the narrow transmission band of one microcavity would drastically limit the light available as input for the next. As an alternative, microcavity-coupled 2-D PhC waveguide structures potentially have significant utility.<sup>53</sup> 2-D PhC waveguides are created by introducing a linear defect (i.e. by eliminating single or multiple rows of air holes from the crystal lattice) into the crystal. The propagation of light in such 2-D PhC slab waveguides is confined by the PBG in the periodicity (x-y) plane and by index guiding in the perpendicular (z) direction.<sup>54</sup> Such structures fulfill all three basic criteria for waveguides: they support true guided modes, are single moded for

given frequency ranges and prohibit radiation loss. As a result, PhC waveguiding enables near-perfect transmission to be achieved across resonant cavities and around bends in the waveguide.<sup>55</sup>

PhC waveguides in which one row of air holes have been removed are called w1 waveguides. A microcavity formed by modifying the radius of a single air hole neighboring the w1 PhC waveguide introduces a defect state in the PBG of the crystal. Consequently, for a certain frequency range, light is transmitted through the w1 waveguide at all frequencies except at the microcavity resonance wavelength, where a dip is observed in the output transmission spectrum (as in Figure 4b). By tuning microcavity defect radii and placing multiple PhC structures in series, multiple transmission dips can be obtained in the output spectrum as each microcavity possesses a unique resonant wavelength. For example, we have fabricated devices with three 2D PhC slab waveguides coupled in series, having lattice constants of 372, 377 and 388 nm (Figure 5). The air hole radii are fixed at 111, 114 and 117 nm and the corresponding defect radii are fixed at 73, 75 and 77 nm, respectively. Structures fabricated with these parameters show three resonant dips at wavelengths of 1510, 1531 and 1551 nm in the output transmission spectrum.

Refractive index sensing was demonstrated with the above device by infiltrating water and isopropanol. Based on the observed red-shift, sensitivity was calculated to be 64.5 nm/RIU. For biosensing, the PhC waveguide devices were functionalized with anti-IgG antibodies, and treated with increasing concentrations of human IgG molecules as the target protein. A red-shift of 3.5 nm was observed after IgG binding for all three resonant wavelengths, demonstrating that all three waveguide-coupled 2-D PhCs responded as expected in a redundant or “error-corrected” fashion.<sup>56</sup> No response was observed in the presence of an equivalent concentration of BSA, confirming an IgG-specific signal. Fitting the IgG concentration-dependent response of the device to a Langmuir adsorption isotherm provided a dissociation constant ( $K_D$ ) for the IgG – anti IgG interaction in good agreement with that reported in the literature. The sensitivity of the device was estimated to be  $\sim 2 \times 10^5$  nm/M. If one assumes that the electric field intensity (>50%) is mostly confined in the defect hole (lower dielectric) as well as the surrounding four holes, direct light-matter interaction in this portion of the devices suggests the detection limit may be estimated to be only 1.5 fg IgG.

Other PhC waveguide structures are also possible. For example, PhC waveguide based drop filters have been investigated for RI sensing and detection of BSA physisorption.<sup>57</sup> Two types of defect nanocavities (L3 and H1-r) were embedded between two spatially separated w1 PhC waveguides to evanescently route light at the cavity mode. The L3 cavity had three missing air holes, while the H1-r cavity included a tuned radius of a single hole. The PhC devices were fabricated on SOI wafers with a Si device thickness of 300 nm. Free-standing membranes were employed in the actual detection. When tested with liquids of different relative refractive indices, the RI sensitivity was estimated to be 0.018 and 0.006 nm per RIU with the L3 and H1-r cavities, respectively. Similarly, nonspecific physical adsorption of BSA on the microcavity sensor surface influenced the microcavity mode wavelength resulting in a total red-shift of 1.73 nm. The evanescent excitation of the cavity modes resulted in a detection limit of  $4.0 \pm 0.6$  fg of BSA.

Simple planar w1 PhC waveguides lacking defects have also been explored for sensing.<sup>58,59</sup> Here, the PhC waveguides were designed to have a single mode at low frequencies, with the mode cutoff falling inside the PBG. This resulted in an abrupt drop of output power in the transmission spectrum. The shift in the position of the drop, rather than in an absorbance initiated by a defect, was used as evidence for detection. Bulk RI sensing and an RI sensitivity of 88 nm/RIU has been demonstrated with this device. Binding of streptavidin to biotin probes on the sensor surface was also monitored, with a 2.5 nm streptavidin film

producing a 0.86 nm cut-off red shift. An interesting observation in this work was that shrinking rather than eliminating a row of holes in a w1 waveguide provided a device with a significantly improved (120 nm/RIU) bulk sensitivity.

Alternatively, incorporation of a slotted waveguide into a 2-D PhC has been proposed as a strategy for increasing device sensitivity.<sup>60</sup> Initial fabrication attempts provided a device with a high Q (50,000) and high refractive index sensitivity (1500 nm/RIU, as tested with glucose solutions of various concentration). While the authors cautioned that the high RIU sensitivity could be in part due to changes in solution wetting properties as a function of sugar concentration, the performance is nevertheless intriguing. Subsequent studies have demonstrated integration of an analogous device into a microfluidic channel, allowing real-time detection of avidin-biotin binding.<sup>61</sup> A similarly high RIU sensitivity has been reported for 2-D PhC optical fibers, in which an array of air holes running along the fiber axis is used to confine light in the fiber core.<sup>62,63</sup>

A 2-D polymer PhC been described and used for reflectometric detection of influenza virus in human saliva.<sup>64</sup> PhCs with different periodicities were fabricated onto a cyclo-olefin polymer film using a nanoimprint lithographic process. Optical characterization as well as optical detection were performed in the visible region (400–800 nm) using a portable UV-VIS spectrophotometer. The reflectometric detection of the influenza virus was based on the structural color changes in the 2D-PhCs in the visible region, and provided a detection limit of 1 ng/ml of influenza virions.

## Other 2D PhC Designs

Several other PhC geometries have been proposed for sensing applications, but not yet tested experimentally. One such structure is a PhC based nano-ring resonator. This structure would be formed by removing holes of a hexagon from a 2D PhC slab in a hexagonal lattice. The authors computationally optimized the performance of the nano-ring resonator by varying the ring radius and the coupling distance, while maintaining the PhC periodicity at 410 nm. This yielded a predicted Q-factor of the resonator structure between 2400 and 3200, and a predicted minimum detectable weight of biomolecules to be 0.2 fg.<sup>65,66</sup> In a related study, a dual PhC microcavity coupled to a stadium shaped ring resonator has been proposed. This design would provide a large sensing area relative to single ring-resonator sensors. Simulations suggest that the RI sensitivity of the device would be on the order of  $3.0 \times 10^{-5}$ .<sup>67</sup>

## Discussion and outlook

In this article we have highlighted recent progress in the use of 1-D and 2-D PhC structures for label-free optical sensing. As we have seen, numerous configurations of 1-D and 2-D PhCs have been created, and some (particularly 1-D PhCs in the out-of-plane detection mode) have successfully made the transition to commercial products. Although many of the experiments described should be regarded as being at the “proof of concept” stage (and reported limits of detection and quantitation should be viewed in that light), and therefore considerable development work remains, several potential advantages of 1-D and 2-D PhC structures over well-developed counterparts such as surface plasmon resonance (SPR) and interferometry-based sensing methods can be highlighted:

- High-throughput applications requiring microwell-plate compatibility and low cost are ideally suited to out-of-plane 1D PhC approaches such as the BIND and EPIC systems. Indeed, such applications have driven their success as commercial products.



- Sensing applications in which sample filtration is potentially useful (for example, whole blood assays) may be well suited to porous silicon based sensors, since the sensor matrix itself can act as a filter.
- 1D PhCs encoded in silicon microparticles are useful in many of the same sensing applications being addressed with (for example) metal and semiconductor nanoparticles. The ability of silicon to degrade *in vivo* into low-toxicity products is a clear advantage here.
- In many PhC structures, the electric field is strongly confined to small modal volumes, facilitating strong light-matter interaction. As a consequence, PhC structures require very small volume of samples (in the order of femtoliters) to detect any analyte of interest and as discussed above can potentially achieve exceptionally high sensitivity. Combined with the fact that both 1-D and 2-D PhC structures have overall dimensions on the order of microns, and many of these structures can be operated in planar formats where the device, the excitation light source as well as the detector are in the same plane, PhC structures may prove particularly suitable for on-chip applications.
- The very small active sensing area of 2D PhCs suggests these may also prove ideal in cases where conservation of the capture molecule is essential.
- 2D PhCs can potentially provide ultra high-sensitivity detection (single particle), a performance beyond the capability of most commercially available sensors.
- Finally, PhC structures exhibit a PBG that can be tuned by changing the periodicity of the structure or the refractive index contrast of the dielectric material. This PBG tunability can be exploited in sensing applications as one can choose any range of working excitation frequency from UV to IR simply by altering the periodicity or the dielectric material type of the PhC structure.

Given these characteristics and the early experimental successes described above, what does the future hold for PhC sensors? We can anticipate that several areas of research and development will be important in the next few years, including:

- More thorough evaluation of the performance of PhC sensors in complex matrices such as serum and plasma: detection of analytes in “real” biological solutions obviously constitutes a significantly greater challenge to the sensor than does a purified analyte in buffer.
- Along these lines, the issue of specificity is a potential concern with any “label-free” technique, since capture of any mass on the sensor leads to a signal and there is no secondary antibody (for example) to ensure specificity (we make a distinction here with “self-labeled” sensors such as those employing immobilized DNA hairpins<sup>68</sup>). In the context of 1-D PhC structures, careful control experiments have been carried out with doped and un-doped samples to verify the effect. Considerable work in this area, however, remains to be done for 2-D PhCs.
- Integration with microfluidics, and other strategies for bringing rare targets to the active sensing area: While 2D PhCs have extraordinarily high theoretical sensitivities, this capability is wasted if analyte diffusion to the active sensing area is limiting.<sup>69</sup> Thus, we anticipate that a key research opportunity in this field will be the development of methods to overcome the diffusion limit, and to maximize the fraction of analyte in solution captured at the active sensing area(s). Optofluidic strategies are one potentially attractive approach in this regard.<sup>70</sup>
- Development of strategies for simplifying fabrication: 1D PhCs for out-of-plane detection are manufacturable on a large scale, and as described above are at the

core of two commercial technologies. For 2D PhCs, current fabrication methods for most of the structures reported to date rely on complex, time-consuming processes such as e-beam lithography. In addition to the cost and relatively slow speed of e-beam, variability in “hole” size in the e-beam lithography process contributes to the relatively low Q-factor of these devices, as well as measurement variability. Improvement of the fabrication precision can potentially improve both the sensitivity of the device and its quantitative measurement accuracy. Therefore, for these sensors to have utility in the commercial sector, significant improvements in their fabrication will need to be made. One possibility is to employ more highly parallel processes such as deep UV photolithography.

- Independently addressing multiple 2D PhCs on a single chip. The waveguide-coupled 2D PhCs described above can be readily configured for multianalyte sensing. Functionalization of individual nanocavities with different capture molecules has yet to be demonstrated, however, and both top-down and bottom-up strategies will need to be examined.

The breadth of configurations, materials, and application spaces explored by researchers engaged in the study of PhC structures suggests that these devices have a vibrant future as objects of fundamental study (understanding the interactions of light with matter) and as central components in the production of novel biosensors and diagnostic tools.

## Acknowledgments

Support from the NIH (R01A108077-01, via NIAID, NIBIB, and NIGMS) is gratefully acknowledged. We thank James Baker and Mark Lifson (University of Rochester) for detailed discussions during the preparation of this manuscript.

## References

1. Friedly G. *J Med Technol.* 1985; 1:823–833.
2. Saiki H, Scharf S, Faloona F, Mullis K, Horn G, Erlich H, Arnheim N. *Science.* 1985; 230:1350–1354. [PubMed: 2999980]
3. (a) Goddard JP, Reymond JL. *Trends Biotechnol.* 2004; 22:363–370. [PubMed: 15245909] (b) Kricka LJ. *Clin Biochem.* 1993; 26:325–331. [PubMed: 8299202] (c) Visor GC, Schulman SG. *J Pharm Sci.* 1981; 70:469–475. [PubMed: 7017106]
4. (a) Washburn AL, Bailey RC. *Analyst.* 2011; 136:227–236. [PubMed: 20957245] (b) Fan X, White IM, Shopova SI, Zhu H, Suter JD, Sun Y. *Anal Chim Acta.* 2008; 620:8–26. [PubMed: 18558119]
5. Yablonovitch E. *Phys Rev Lett.* 1987; 58:2059. [PubMed: 10034639]
6. John S. *Phys Rev Lett.* 1987; 58:2486. [PubMed: 10034761]
7. 1-D and 2-D PhC structures are from the authors' laboratories; the 3-D PhC is described in: Miyake M, Chen YC, Braun PV, Wiltzius P. *Adv Mater.* 2009; 21:3012–3015.
8. Selected reviews of the use of porous silicon in sensing include: Jane A, Dronov R, Hodges A, Voelcker NH. *Trends Biotechnol.* 2009; 27:230–239. [PubMed: 19251329] Sailor MJ. *ACS Nano.* 2007; 1:248–252. [PubMed: 19206674] Miller BL, Zourob M, Lakhtakia A. *Optical Guided Wave Sensors and Biosensors.* 2010Springer:3–25.
9. Ulhir A. *Bell Syst Tech J.* 1956; 35:333.
10. Turner TR. *J Electrochem Soc.* 1958; 105:402.
11. Canham PC. *Appl Phys Lett.* 1990; 57:1046.
12. Janshoff A, Dancil KPS, Steinem C, Greiner DP, Lin VSY, Gurtner C, Motesharei K, Sailor MJ, Ghadiri MR. *J Am Chem Soc.* 1998; 120:12108–12116.
13. Fauchet PM. *Semiconductors and Semimetals.* 1997; 49:205–252.
14. Cazzanelli M, Vinegoni C, Pavesi L. *J Appl Phys.* 1999; 85:1760–1764.
15. Chan S, Fauchet PM, Li Y, Rothberg LJ, Miller BL. *Physica Status Solidi A.* 2000; 182:541–546.

16. Chan S, Horner SR, Miller BL, Fauchet PM. *J Am Chem Soc.* 2001; 123:11797–11798. [PubMed: 11716737]
17. Hubbard RD, Horner SR, Miller BL. *J Am Chem Soc.* 2001; 123:5810–5811. [PubMed: 11403619]
18. Ouyang H, Christophersen M, Viard R, Miller BL, Fauchet PM. Macroporous Silicon Microcavities for Macromolecule Detection. *Adv Func Mat.* 2005; 15:1851–1859.
19. DeLouise LA, Fauchet PM, Miller BL, Pentland AP. Hydrogel-Supported Optical Microcavity Sensors. *Advanced Materials.* 2005; 17:2199–2203.
20. Bonanno LM, DeLouise LA. *Anal Chem.* 2010; 82:714–722. [PubMed: 20028021]
21. Bonanno LM, Kwong TC, DeLouise LA. *Anal Chem.* 2010; 82:9711–9718. [PubMed: 21062030]
22. Link JR, Sailor MJ. *Proc Natl Acad Sci USA.* 2003; 100:10607–10610. [PubMed: 12947036]
23. Orosco MM, Pacholski C, Sailor MJ. *Nature Nanotech.* 2009; 4:255–258.
24. Ciampi S, Böcking T, Kilian KA, Harper JB, Gooding JJ. *Langmuir.* 2008; 24:5888–5892. [PubMed: 18452318]
25. Guan B, Magenau A, Kilian KA, Ciampi S, Gaus K, Reece PJ, Gooding JJ. *Faraday Discuss.* 2011; 149:301–317. [PubMed: 21413188]
26. Guo Y, Ye JY, Divin C, Huang B, Thomas TP, Baker J, Norris TB. *Ana Chem.* 2010; 82:5211–5218.
27. Guo Y, Divin C, Myc A, Terry FL, Baker JR, Norris TB, Ye JY. *Opt Express.* 2008; 16:11741–11749. [PubMed: 18679444]
28. Mandal S, Goddard JM, Erickson D. *Lab Chip.* 2009; 9:2924–2932. [PubMed: 19789745]
29. Cunningham BT. *J Assoc Lab Aut.* 2010; 15:120–135.
30. Cunningham B, Lin B, Qiu J, Li P, Pepper J, Hugh B. *Sens Act B- Chem.* 2002; 85:219–226.
31. Chan LL, Pineda M, Heeres JT, Hergenrother PJ, Cunningham BT. *ACS Chem Biol.* 2008; 3:437–448. [PubMed: 18582039]
32. Chan LL, Gosangari SL, Watkin KL, Cunningham BT. *Sens Act B: Chem.* 2008; 132:418–425.
33. Cunningham BT, Laing L. *Expert Rev Proteomics.* 2006; 3:271–281. [PubMed: 16771700]
34. Pineda MF, Leo LYC, Kuhlenschmidt T, Choi CJ, Kuhlenschmidt M, Cunningham BT. *IEEE Sensors J.* 2009; 9:470–477.
35. Cunningham BT, Li P, Schulz S, Lin B, Baird C, Gerstenmaier J, Genick C, Wang F, Fine E, Laing L. *J Biomol Screening.* 2004; 9:481–490.
36. Fang Y, Ferrie AM, Li G. *FEBS Lett.* 2005; 579:4175–4180. [PubMed: 16038906]
37. Fang Y, Ferrie AM, Fontaine NH, Mauro J, Balakrishnan J. *Biophys J.* 2006; 91:1925–1940. [PubMed: 16766609]
38. Heeres JT, Kim SH, Leslie BJ, Lidstone EA, Cunningham BT, Hergenrother PJ. *J Am Chem Soc.* 2009; 131:18202. [PubMed: 19968284]
39. Mathias PC, Ganesh N, Chan LL, Cunningham BT. *Appl Opt.* 2007; 46:2351–2360. [PubMed: 17415405]
40. Kim, S-min; Zhang, W.; Cunningham, BT. *Appl Phys Lett.* 2008; 93:143112.
41. Joannopoulos, JD.; Johnson, SG.; Winn, JN.; Meade, RD. *Photonic Crystals: Molding the Flow of Light.* 2. Princeton University Press; 2008.
42. Prather, DW.; Sharkawy, A.; Shi, S.; Murakowski, J.; Schneider, G. *Photonic Crystals, Theory, Applications and Fabrication.* 1. Wiley; 2009.
43. Kippenberg TJ, Spillane SM, Vahala KJ. *Appl Phys Lett.* 2004; 85:6113.
44. Adawi AM, Murshidy MM, Fry PW, Lidzey DG. *ACS Nano.* 2010; 4:3039–3044. [PubMed: 20499907]
45. Washburn AL, Luchansky MS, Bowman AL, Bailey RC. *Anal Chem.* 2010; 82:69–72. [PubMed: 20000326]
46. Vollmer F, Arnold S, Keng D. *Proc Natl Acad Sci USA.* 2008; 105:20702–20704.
47. Chow E, Grot A, Mirkarimi LW, Sigalas M, Girolami G. *Opt Lett.* 2004; 29:1093–1095. [PubMed: 15181996]
48. Altug H, Vuckovic J. *Opt Lett.* 2005; 30:982–984. [PubMed: 15906977]

49. Altug H, Vu kovi J. *Appl Phys Lett*. 2004; 84:161.
50. Lee MR, Fauchet PM. *Opt Express*. 2007; 15:4530–4535. [PubMed: 19532700]
51. Lee MR, Fauchet PM. *Opt Lett*. 2007; 32:3284–3286. [PubMed: 18026281]
52. Zlatanovic S, Mirkarimi LW, Sigalas MM, Bynum MA, Chow E, Robotti KM, Burr GW, Esener S, Grot A. *Sens Actuat B*. 2009; 141:13–19.
53. Pal S, Guillermain E, Sriram R, Miller B, Fauchet PM. *Proc SPIE*. 2010; 7553:755304–1.
54. Liu K, Yuan XD, Ye WM, Zeng C. *Opt Comm*. 2009; 282:4445–4448.
55. Johnson SG, Villeneuve PR, Fan S, Joannopoulos JD. *Phys Rev B*. 2000; 62:8212–8222.
56. Pal S, Guillermain E, Sriram R, Miller BL, Fauchet PM. *Biosens Bioelectron*. 2011; 26:4024–4031.
57. Dorfner D, Zabel T, Hürlimann T, Hauke N, Frandsen L, Rant U, Abstreiter G, Finley J. *Biosens Bioelectron*. 2009; 24:3688–3692. [PubMed: 19501502]
58. Skivesen N, Têtu A, Kristensen M, Kjems J, Frandsen LH, Borel PI. *Opt Express*. 2007; 15:3169–3176. [PubMed: 19532555]
59. Buswell SC, Wright VA, Buriak JM, Van V, Evoy S. *Opt Express*. 2008; 16:15949–15957. [PubMed: 18825232]
60. Di Falco A, O'Faolain L, Krauss TF. *Appl Phys Lett*. 2009; 94:063503.
61. Scullion MG, Di Falco A, Krauss TF. *Biosens Bioelectron*. 2011; 27:101–105. [PubMed: 21764290]
62. Rindorf L, Bang O. *Opt Lett*. 2008; 33:563–565. [PubMed: 18347710]
63. Rindorf L, Jensen JB, Dufva M, Pedersen LH, Højby PE, Bang O. *Opt Express*. 2006; 14:8224–8231. [PubMed: 19529196]
64. Endo T, Ozawa S, Okuda N, Yanagida Y, Tanaka S, Hatsuzawa T. *Sens Act B: Chem*. 2010; 148:269–276.
65. Hsiao FL, Lee C. *Procedia Chem*. 2009; 1:417–420.
66. Hsiao, F-li; Lee, C. *IEEE Sensors J*. 2010; 10:1185–1191.
67. Kim H-S, Oh G-Y, Choi Y-W. *Opt Eng*. 2010; 49:054401.
68. Peng HI, Strohsahl CM, Miller BL. *Lab on a Chip*. 2012; 12:1089–1093. [PubMed: 22301735]
69. Sheehan PE, Whitman LJ. *Nano Lett*. 2005; 5:803–807. [PubMed: 15826132]
70. Chen YF, Serey X, Sarkar R, Chen P, Erickson D. *Nano Lett*. 2012; 12:1633–1637. [PubMed: 22283484]

## Biography

Biography: Sudeshna Pal was a postdoctoral research associate in the Department of Electrical & Computer Engineering at the University of Rochester. She is currently continuing postdoctoral research at the University of Central Florida. Her areas of research include biosensors, biophotonics, and bio-inspired controls. Philippe Fauchet is Dean of the School of Engineering and Professor of Electrical Engineering at Vanderbilt University. His research interests are in photonics, energy, and the semiconductor/biology interface, all using silicon-based nanoscience and nanotechnology. Benjamin Miller is Professor of Dermatology, Biochemistry and Biophysics, and Biomedical Engineering at the University of Rochester. His research is focused on the development of methods for sequence-selective recognition of RNA, and on optical biosensors and diagnostic devices.

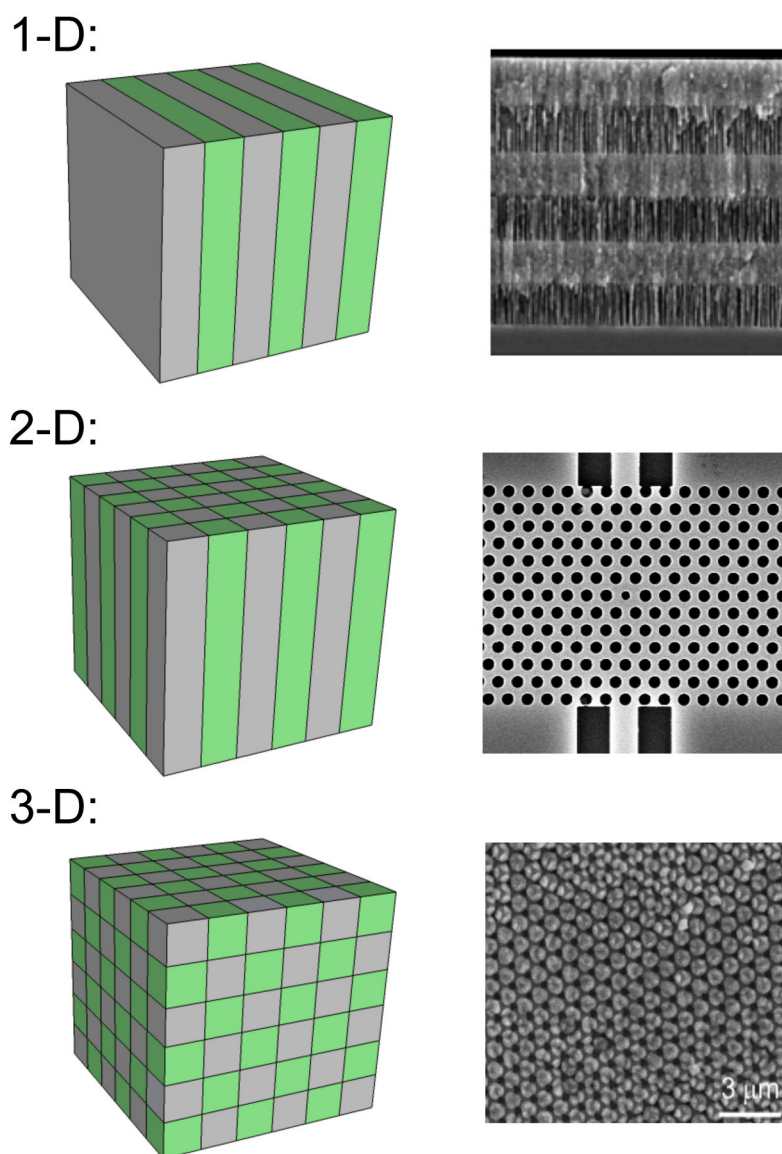


**Figure 1.** 1-, 2-, and 3-D photonic crystals. Schematics on the left indicate the alternating patterns of high and low refractive index materials, while scanning electron micrographs of representative examples of each type of PhC are on the right (top: a Bragg mirror in porous silicon; middle: a 2-D PhC created on a silicon-on-insulator chip via E-beam lithography; bottom: top surface of an inverse 3D copper(I) oxide PhC<sup>7</sup>).

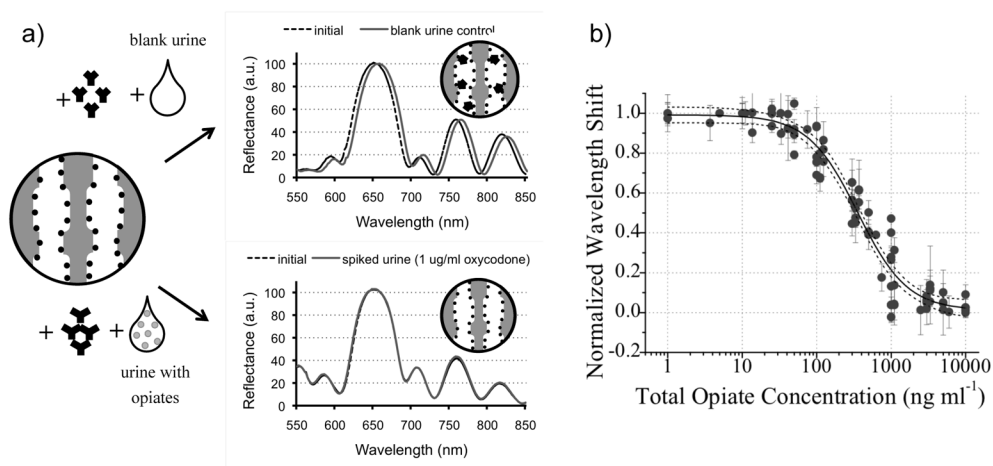


**Figure 2.**

Preliminary validation of a 1-D PhC sensor fabricated from porous silicon in a clinical context. (a) Treatment of an opiate-functionalized sensor with anti-opiate antibodies and blank urine causes a red-shift due to antibody binding (top), while urine containing opiates competes for antibody binding and reduces sensor response (bottom). (b) Calibration curve for sensor response. Adapted from reference 21.

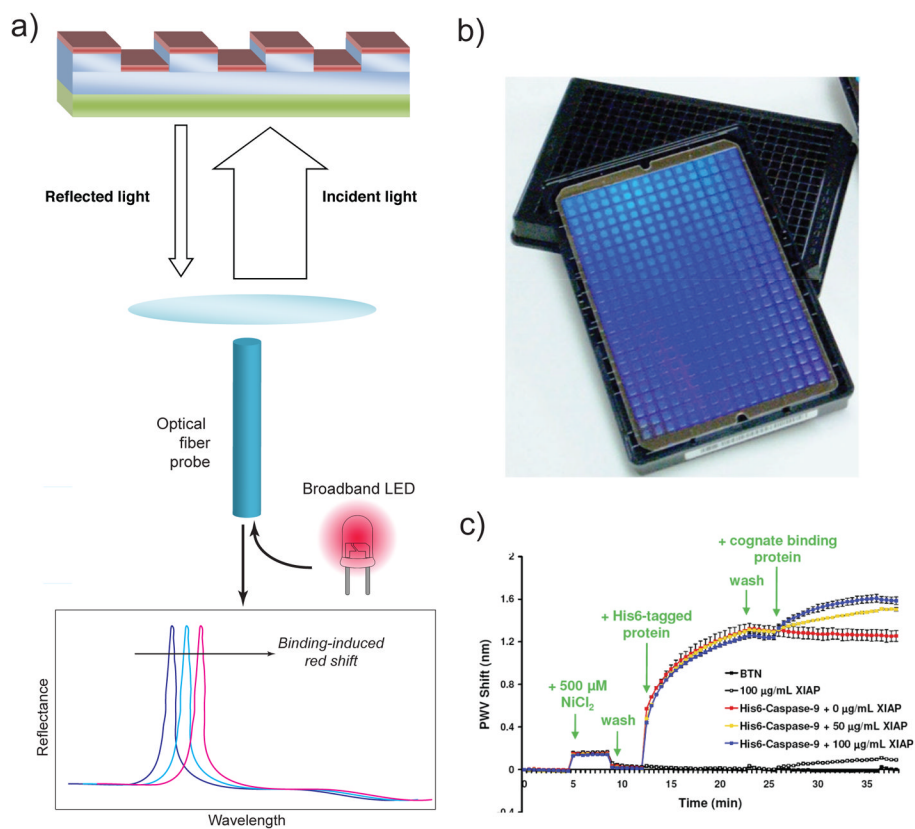


**Figure 3.** 2-D PhCs for out-of-plane detection. (a) Materials system and schematic of measurement setup. (b) A commercial 384-well plate incorporating 2D PhCs. (c) Demonstration of real-time detection of protein-protein binding in a 384-well format<sup>38</sup>.

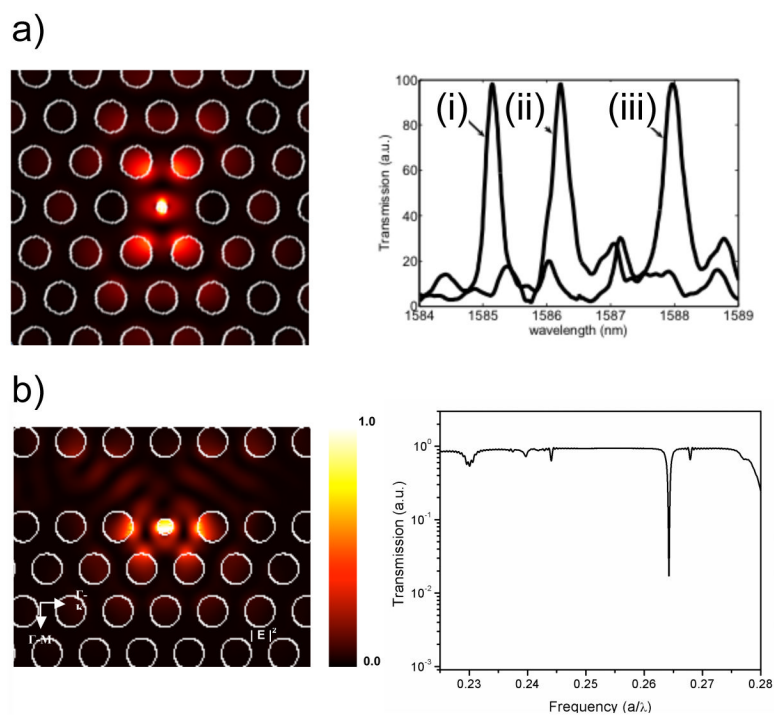


**Figure 4.** Calculated electric field profiles (left) and experimental spectra (right) for (a) 2D PhC microcavity and (b) w1 waveguide-coupled PhC structures. Changes in peak position in (a) represent: the initial experimental response of the microcavity (i), and sequential covalent modification with glutaraldehyde (ii) and bovine serum albumin (iii) (adapted from reference 50).



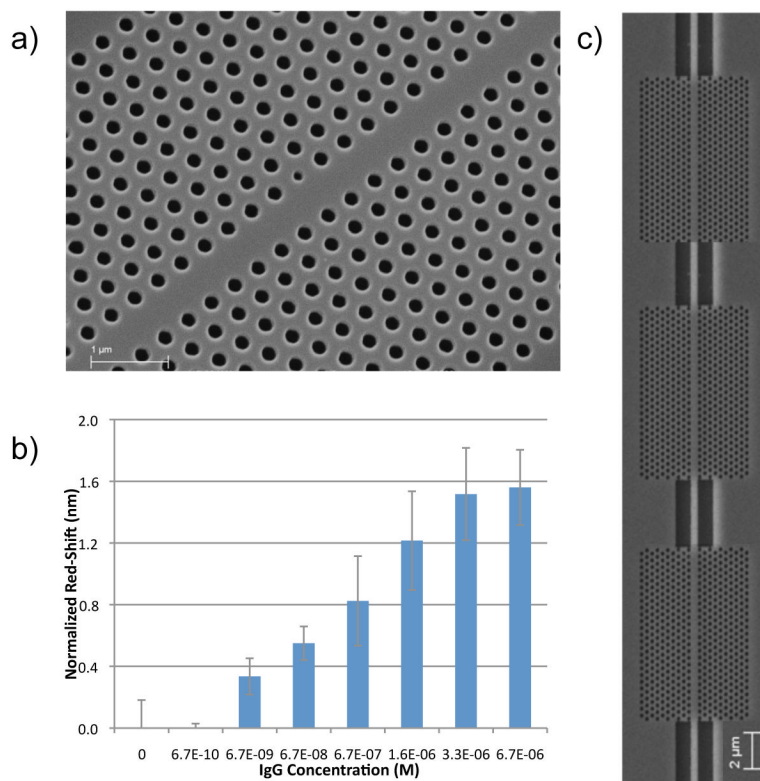


**Figure 5.** (a) SEM image of a w1 waveguide-coupled 2-D PhC used for IgG biosensing after functionalization with an anti-IgG antibody. (b) Concentration-dependent response of this sensor to IgG (note that in some cases neighboring concentrations are indistinguishable from one another given overlapping error bars). (c) SEM image of three w1 waveguide-coupled 2-D PhCs in series (adapted from reference 56).